

---

# 1 Hydrological drought forecasting under a changing environment 2 in the Luanhe River basin

3 Min Li<sup>1,2</sup>, Mingfeng Zhang<sup>1</sup>, Runxiang Cao<sup>3</sup>, Yidi Sun<sup>1</sup>, Xiyuan Deng<sup>4,5</sup>,  
4 (<sup>1</sup>College of Hydraulic Science and Engineering, Yangzhou University, Yangzhou,  
5 China, 225000; <sup>2</sup>State Key Laboratory of Hydraulic Engineering Simulation and Safety,  
6 Tianjin University, Tianjin, China, 300072; <sup>3</sup>College of Water Resources, North China  
7 University of Water Resources and Electric Power, Zhengzhou, China, 450046;  
8 <sup>4</sup>Nanjing Hydraulic Research Institute, Nanjing, China, 210029; <sup>5</sup>State Key Laboratory  
9 of Hydrology-Water Resources and Hydraulic Engineering, Nanjing, China, 210029)

10 **Abstract:** Forecasting the occurrence of hydrological drought according to a  
11 forecasting system is an important disaster reduction strategy. In this paper, a new  
12 drought prediction model adapted to changing environments was constructed. Taking  
13 the Luan River basin in China as an example, first, nonstationarity analysis of  
14 hydrological sequences in the basin was carried out. Then, conditional distribution  
15 models with the human activity factor as an exogenous variable were constructed to  
16 forecast hydrological drought based on meteorological drought, and the results were  
17 compared with the traditional normal distribution model and conditional distribution  
18 model. Finally, a scoring mechanism was applied to evaluate the performance of the  
19 three drought forecasting models. The results showed that the runoff series of the  
20 Luanhe River basin from 1961 to 2010 were nonstationary; moreover, when human  
21 activities were not considered, the hydrological drought class tended to be the same as  
22 the meteorological drought class. The calculation results of the models involving *HI* as  
23 an exogenous variable were significantly different from the models that did not consider  
24 human activities. When the current drought class tended towards less severe or normal,  
25 the meteorological drought tended to turn into more severe hydrological drought with  
26 the increase in human index values. According to the scores of the three drought  
27 forecasting models, the conditional distribution models involving the human index can  
28 further improve the forecasting accuracy of drought in the Luanhe River basin.

29 **Keywords:** Changing environment; Drought forecasting; Human activity factor;  
30 Luanhe River basin

31 **Acknowledgements:** This work was supported by the State Key Laboratory of  
32 Hydraulic Engineering Simulation and Safety (Tianjin University) program (No.  
33 HESS-2206 and No. HESS-2222).

---

1 Corresponding author: Min Li                      Mail: [limintju@126.com](mailto:limintju@126.com)  
Xiyuan Deng    Mail: [xydeng@nhri.cn](mailto:xydeng@nhri.cn)

---

## 35 **1 Introduction**

36 Typically, meteorological drought is regarded as the beginning of a drought event;  
37 after the occurrence of meteorological drought, other drought phenomena occur, such  
38 as hydrological drought (Miriam et al., 2018; Fuentes et al., 2022; Wang et al., 2021).  
39 However, there is a delay period from meteorological drought to hydrological drought  
40 (Ding et al., 2021; Xu et al., 2019; Charles, 2017; Carmelo and Jürgen, 2018). Therefore,  
41 the occurrence of hydrological drought can be forecasted according to meteorological  
42 drought monitoring. Accurate hydrological forecast information is beneficial to reduce  
43 the losses caused by hydrological drought (Behzad and Hamid, 2019; Melanie et al.,  
44 2018 Dixit et al.,2022; Muhammad et al.,2020).

45 To identify the drought characteristics of the region, scholars have developed  
46 drought indices. For example, the standardized precipitation index (SPI) is typically  
47 used to identify and capture the characteristics of meteorological drought (McKee,  
48 1993). Considering the influence of precipitation and temperature, Vicente-Serrano et  
49 al. (2010) proposed the standardized precipitation evapotranspiration index (SPEI) to  
50 characterize meteorological drought. The standardized runoff index (SRI), which  
51 focuses on the surface runoff of catchments, is typically used to indicate hydrological  
52 drought (Shukla, 2008). Aghelpour and Varshavian (2021) proposed the multivariate  
53 standardized precipitation index (MSPI) to forecast hydrological drought in Iran.

54 Statistical technology is an effective prediction method that has been widely used  
55 in drought forecasting in recent years (Alquraish et al., 2021; Abbasi et al., 2021;  
56 Bagher et al., 2013). For instance, neural network models have been proposed to  
57 combine multiple data for drought prediction (Mehdi et al., 2016; Maryam et al., 2017;  
58 Ahnadi et al., 2011), and time series models can be used to analyse the variation in time  
59 series such as rainfall and runoff to achieve drought prediction (Mohammad et al., 2020;  
60 Natsagdorj et al., 2021; Stojković et al., 2020). The conditional probability model was  
61 proposed by Cancelliere et al. (2007) and developed for drought forecasting by  
62 Bonaccorso et al. (2015). Bonaccorso et al. (2015) showed that the conditional  
63 probability model can calculate the transition probabilities from the current drought

---

64 index values to the future drought classes, and this is a more robust method that can be  
65 used to forecast drought than the traditional probability prediction models (such as the  
66 multivariate normal distribution model and Markov method).

67 A change in the environment may lead to the nonstationarity of the relationship  
68 between hydrological series (for example, precipitation and runoff series), which also  
69 occurs in the Luanhe River basin (Wang et al., 2018; Li et al., 2015; Wang et al., 2016).  
70 Traditional drought prediction methods need to be further improved to adapt to  
71 nonstationary conditions (Wang et al., 2022; Zhao et al., 2018; Chen et al. (2021)). Ren  
72 et al. (2017) found that the conditional distribution model using large-scale climatic  
73 indices as covariates can improve the accuracy of meteorological drought forecasting  
74 in the Luanhe River basin. Although some progress has been made in the study of  
75 drought forecasting, there are relatively few studies considering the impact of the  
76 changing environment.

77 In this paper, to analyse the impact of human activities on hydrological drought,  
78 we constructed the human activity index (*HI*) based on the restoration method.  
79 Subsequently, conditional distribution models with the *HI* as the exogenous variable  
80 were developed to forecast hydrological drought based on meteorological drought,  
81 and then the results were compared with the traditional normal distribution model and  
82 conditional distribution model; as a result, the impact of human activities on transition  
83 probabilities was illustrated. A scoring mechanism was applied to the evaluation of the  
84 three probability models.

85 In addition to the introduction, this paper contains the following sections. Section  
86 2 introduces the study area and data. Section 3 briefly describes the methods used in  
87 the research. Section 4 introduces the model construction and calculation results and  
88 analyses the results. Section 5 presents the prospects.

## 89 **2 Study area and data**

90 The Luanhe River basin, located in the subtropical monsoon region, covers an area  
91 of approximately 33700 square kilometres. Its geographical location is shown in Figure  
92 1. Due to the influence of geographical location and topography, the annual average

---

93 north–south temperature difference in the basin is 11.5 °C, and the annual rainfall  
94 distribution is uneven. Less rain in spring and winter makes the area prone to  
95 meteorological drought and hydrological drought, while there is relatively more rainfall  
96 in summer. The average rainfall in summer is approximately 200-560 mm, resulting in  
97 highly variable annual runoff in the basin. The concentrated rainfall in summer has also  
98 become one of the remarkable features of the climate in this area. In recent years, the  
99 precipitation and inflow of the Luanhe River basin have gradually decreased, the water  
100 level of the Panjiakou Reservoir in the lower reaches of the basin has decreased, the  
101 runoff has decreased, and the frequency of meteorological drought and hydrological  
102 drought has significantly increased. Especially after entering the 21st century, the river  
103 basin has exhibited continuous drought and even extreme drought. With the change in  
104 the global climate and the impact of human activities on the basin environment, drought  
105 disasters in the Luanhe River basin occur frequently, causing significant social and  
106 economic losses.

107 Influenced by topography, meteorology, hydrology and hydrogeological  
108 conditions, the spatial distribution of groundwater resources in the Luanhe River basin  
109 is quite different. The recharge and storage conditions of shallow groundwater in plain  
110 areas and intermountain basins are relatively superior, and the content of groundwater  
111 in mountainous areas is relatively small (the area of mountainous areas in the Luanhe  
112 River basin accounts for 98.2%). Therefore, the total amount of water resources in the  
113 Luanhe River basin is mainly considered to be affected by the amount of surface water  
114 resources.

115 In this paper, the monthly rainfall data from 26 stations in the Luanhe River basin  
116 from 1961 to 2010 were provided by the Hebei Provincial Hydrology and Water  
117 Resources Investigation Bureau. The average monthly rainfall data of the area were  
118 obtained by the inverse distance weighting interpolation method. The runoff data from  
119 1961 to 2010 came from the inflow runoff series of the Panjiakou Reservoir. The SPI  
120 and SRI can be calculated for 1-month, 3-month, 6-month, and 12-month time scales  
121 to characterize meteorological drought and hydrological drought based on these data.

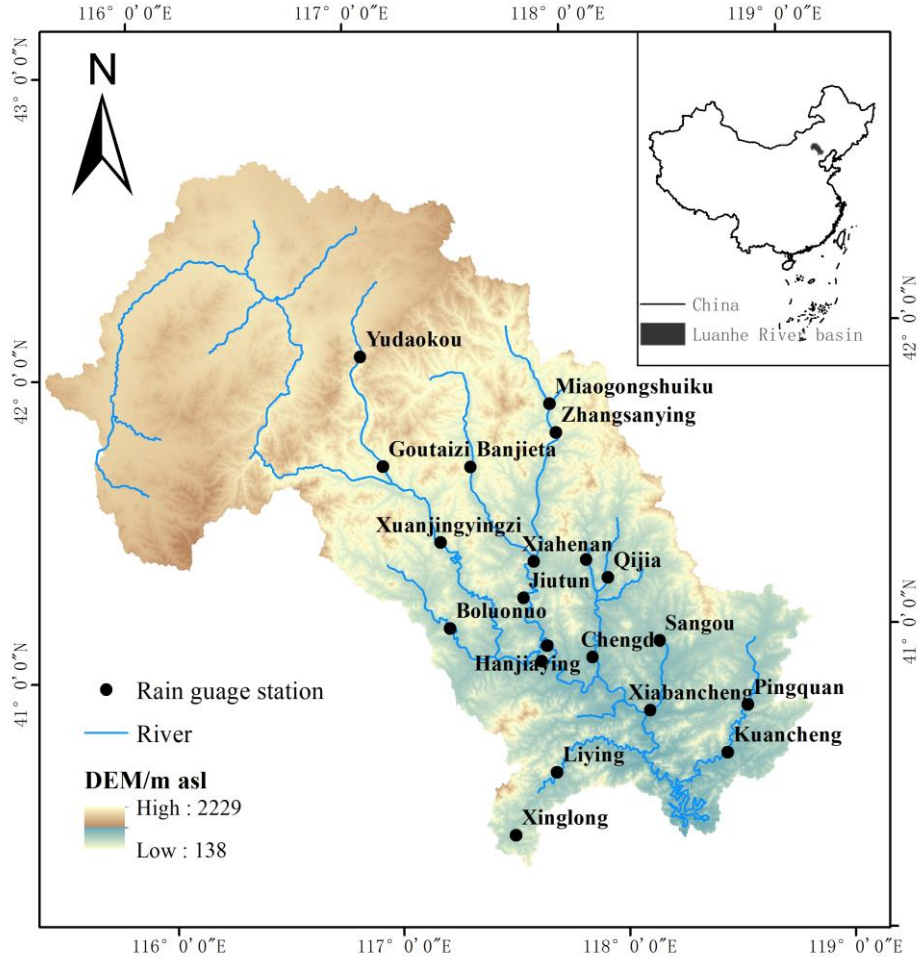


Figure 1 The geographical location of the Luanhe River basin

### 3 Methods

#### 3.1 Nonstationarity test method

In the case of environmental changes, nonstationarity may occur in hydrological series. The Pettitt test, as one of the important methods to test whether there is nonstationarity in time series, can identify whether there are change points in the sample series (Malede et al., 2022). Assuming that the sample sequence is  $x = (x_1, x_2, \dots, x_n)$ , the formula is as follows:

$$U_{t,n} = U_{t-1,n} + \sum_{i=1}^n \text{sgn}(x_t - x_i) \quad (t = 2, 3, \dots, n) \quad (1)$$

$$\text{sgn}(x_t - x_i) = \begin{cases} 1 & x_t - x_i > 0 \\ 0 & x_t - x_i = 0 \\ -1 & x_t - x_i < 0 \end{cases} \quad (2)$$

133 where  $U_{t,n}$  is the test statistic, which indicates the cumulative number of the values  
 134 at time  $t$  greater than or less than the values at time  $i$ . In addition, if  $K_{t_0,n}$  satisfies the  
 135 following:

$$136 \quad K_{t_0,n} = \max |U_{t,n}| \quad (t=1,2,\dots,n) \quad (3)$$

137 Then,  $t_0$  is considered to be the change point, and the cumulative probability of  
 138 possible change is determined by  $K_{t_0,n}$ :

$$139 \quad P_{t_0,n} = 2 \exp\left(-\frac{6K_{t_0,n}^2}{n^3 + n^2}\right) \quad (4)$$

140 Given the significance level  $\alpha = 0.05$ , if  $P_{t_0,n} > 0.95$ , it means that the point is a significant  
 141 change point (Li et al., 2022; Koudahe et al., 2018). Furthermore, combined with the  
 142 Mann-Kendall test, the trend characteristics of the sample series can be obtained  
 143 (Linchao et al., 2018).

144 The sliding T test is a basic method commonly used in statistics. According to the  
 145 mean and variance of the two sample sequences before and after the change points in  
 146 the runoff time series, the two sample sequences are tested (Li et al., 2020):

$$147 \quad t = \frac{\bar{x}_1 - \bar{x}_2}{S \sqrt{\frac{1}{n_1} + \frac{1}{n_2}}} \quad (5)$$

$$148 \quad S = \sqrt{\frac{(n_1 - 1)S_1^2 + (n_2 - 1)S_2^2}{n_1 + n_2 - 2}} \quad (6)$$

$$149 \quad S_1^2 = \frac{1}{n_1 - 1} \sum_{t=1}^{n_1} (x_t - \bar{x}_1)^2 \quad (7)$$

$$150 \quad S_2^2 = \frac{1}{n_2 - 1} \sum_{t=1}^{n_1+n_2} (x_t - \bar{x}_2)^2 \quad (8)$$

151 where the change point is  $x_t$ ,  $n_1$  and  $n_2$  represent the sample size before and after  
 152 the change point, and  $S_1^2$  and  $S_2^2$  represent the variance of the samples before and after  
 153 the change point, respectively. If the  $t$  statistic satisfies  $t > t_\alpha$  at the significance level  
 154 of  $\alpha = 0.05$ , the point can be considered a change point.

---

155 The Spearman correlation test can be applied to test the trend of time series, and  
156 the specific description refers to the article of Bishara and Hittner (2012).

### 157 3.2 Human activity index

158 The rainfall and runoff series of the watershed are usually strongly correlated.  
159 However, under the interference of human activities, the relationship between rainfall  
160 and runoff changes.

161 The double cumulative curve method can test the nonstationarity of the bivariate  
162 correlation between rainfall series and runoff series, and the point where the underlying  
163 surface is significantly altered by human activities can be determined according to the  
164 position of the slope change of the curve. Due to the short data series before and after  
165 the change point (20 years before the change point and 30 years after the change point),  
166 a linear equation was used to fit the relationship between precipitation and runoff.

167 The linear regression relationship of the cumulative rainfall and runoff series can  
168 be calculated according to the following formula:

$$169 \quad \sum x = k \sum y + b \quad (9)$$

170 where  $x$  is the runoff series;  $y$  is the rainfall series;  $k$  is the correlation coefficient of the  
171 regression equation; and  $b$  is the intercept of the regression equation.

172 Human activities are the main reason for the nonstationarity of the runoff series in  
173 the watershed, so the  $HI$  can be constructed to quantify the impact of human activities  
174 on runoff. Based on the linear regression relationship established between the  
175 accumulated precipitation and the accumulated runoff before the change point, the  
176 theoretical runoff sequence during the human activity period can be calculated from the  
177 measured precipitation sequence.  $SRI'$  represents the standardized runoff index value  
178 without human activity interference, and  $SRI$  represents the normalized runoff index  
179 value calculated based on the measured runoff sequence under the disturbance of human  
180 activities. The  $HI$  is obtained by subtracting the theoretical  $SRI'$  and the actual  $SRI$ ,  
181 and the calculation formula is as follows:

$$182 \quad HI = SRI' - SRI \quad (10)$$

183 When  $HI > 0$ , it can be assumed that human activities exacerbate hydrological  
184 drought,  $HI < 0$  means that the actual  $SRI$  is greater than the theoretical  $SRI$  without

185 human activities, and when  $HI=0$ , the watershed is considered undisturbed by human  
 186 activities.

### 187 3.3 Multivariate normal distribution model

188 The SPI is one of the important indicators for evaluating meteorological drought  
 189 in the basin, and the SRI is an important indicator for evaluating hydrological drought  
 190 in the basin. According to the rainfall data and runoff data in the basin, the SPI and SRI  
 191 can be calculated at different time scales. Table 1 provides the drought class  
 192 classification and corresponding SPI values and SRI values (Kolachian and Saghafian,  
 193 2021).

194 Table 1 Drought class classification and corresponding SPI values and SRI values

SPI/SRI values	Class
> -0.99	Normal
-1.00 to -1.49	Moderate
-1.50 to -1.99	Severe
$\leq -2.00$	Extreme

195  
 196 As a traditional drought class forecasting model, the multivariate normal  
 197 distribution model (Model 1) can forecast the future SRI class according to the current  
 198 SPI class. Assuming that the current SPI and SRI series both satisfy a multivariable  
 199 normal distribution, the joint probability density can be expressed as follows (Chang et  
 200 al., 2022):

$$201 \quad f_{Z_{v,\lambda}^{(k)} W_{v,\lambda+M}^{(k)}}(t, s) = \frac{1}{2\pi |\Sigma|} \cdot \exp\left(-\frac{1}{2} \mathbf{X}^T \Sigma^{-1} \mathbf{X}\right) \quad (11)$$

202 where  $\Sigma$  is the covariance matrix, and  $\mathbf{X} = [t, s]^T$ . The form of the covariance  
 203 matrix is as follows:

$$204 \quad \Sigma = \begin{bmatrix} 1 & \text{cov}[Z_{v,\lambda}^{(k)}, W_{v,\lambda+M}^{(k)}] \\ \text{cov}[Z_{v,\lambda}^{(k)}, W_{v,\lambda+M}^{(k)}] & 1 \end{bmatrix} \quad (12)$$

205 Furthermore, according to the joint probability density function of the SPI value  
 206  $Z_{v,\lambda}^{(k)}$  at year  $\nu$  and month  $\lambda$  and the future  $M$  month's SRI value  $W_{v,\lambda+M}^{(k)}$ , the analytical

207 formula of the transition probability of the future SRI drought class can be obtained  
 208 (Zhang et al., 2017):

$$209 \quad P\left[W_{v,\lambda+M}^{(k)} \in C_M\right] = \frac{\iint_{C_N C_M} f_{Z_{v,\lambda}^{(k)} W_{v,\lambda+M}^{(k)}}(t, s) \cdot dt \cdot ds}{\int_{C_N} f_{Z_{v,\lambda}^{(k)}}(t) \cdot dt} \quad (13)$$

210 where  $C_M$  represents the drought class, and  $f_{Z_{v,\lambda}^{(k)}}(t)$  represents the marginal  
 211 density function of  $Z_{v,\lambda}^{(k)}$  in the current  $\lambda$  month.

### 212 3.4 Conditional distribution model

213 The conditional distribution model (Model 2) proposed by Bonaccorso et al.  
 214 (2015) is described as follows: when one group of sample data  $X$  obeys a normal  
 215 distribution and satisfies  $X \sim N(\mu_1, \Sigma_1)$ , and another group of sample data  $Y$  also  
 216 obeys a normal distribution, namely,  $Y \sim N(\mu_2, \Sigma_2)$ , then the total sequence can be  
 217 written as follows:

$$218 \quad B = \begin{bmatrix} X \\ Y \end{bmatrix} \begin{matrix} r \\ p-r \end{matrix} \sim N_p \left( \begin{bmatrix} \mu_1 \\ \mu_2 \end{bmatrix}, \begin{bmatrix} \Sigma_{11} & \Sigma_{12} \\ \Sigma_{21} & \Sigma_{22} \end{bmatrix} \right) \quad (14)$$

219 When sequence  $Y$  obeys a normal distribution, the distribution of sequence  $X$  under  
 220 the  $Y$  condition still satisfies a normal distribution, namely, the distribution of  $(X | Y)$   
 221 is as follows (Gong et al. 2021):

$$222 \quad (X | Y) \sim N(\mu_3, \Sigma_3) \quad (15)$$

223 where  $\mu_3$  represents the expected value under the conditional distribution, and  $\Sigma_3$   
 224 is the conditional covariance matrix:

$$225 \quad \mu_3 = \mu_1 + \Sigma_{12} \Sigma_{22}^{-1} (y - \mu_2) \quad (16)$$

$$226 \quad \Sigma_3 = \Sigma_{11} - \Sigma_{12} \Sigma_{22}^{-1} \Sigma_{21} \quad (17)$$

227 Then, the probability of the current SPI value transitioning to the future SRI  
 228 drought class can be deduced as follows (Ren et al., (2017)):

$$229 \quad P\left[W_{v,\lambda+M} \in C_M / Z_{v,\lambda} = z_0\right] = \int_{C_{Mi}}^{C_{Ms}} \frac{1}{\sqrt{2\pi}\sigma_Z} e^{-\frac{1}{2}\left(\frac{x-\rho z_0}{1-\rho^2}\right)^2} dx \quad (18)$$

230 where  $Z_{v,\lambda}$  represents the SPI value of the current month  $\lambda$ ,  $W_{v,\lambda+M}$  represents the  
 231 SRI value of the  $\lambda + M$  month,  $C_{Ms}$  and  $C_{Mi}$  are the upper and lower limits of drought  
 232 class  $C_M$ , and the correlation coefficient between the current SPI value and the future  
 233 SRI value is  $\rho$ . Furthermore, the current SPI and future SRI can be expressed as the  
 234 standard normal cumulative distribution function  $\Phi$ :

$$235 \quad P\left[W_{v,\lambda+M} \in C_M \mid Z_{v,\lambda} = z_0\right] = \Phi\left[\frac{C_{Ms} - \rho \cdot z_0}{1 - \rho^2}\right] - \Phi\left[\frac{C_{Mi} - \rho \cdot z_0}{1 - \rho^2}\right] \quad (19)$$

236 The calculation of the correlation coefficient  $\rho$  is as follows:

$$237 \quad \rho = \frac{\text{cov}[Z_{v,\lambda}^{(k)}, W_{v,\lambda+M}^{(k)}]}{\sqrt{\text{var}(Z_{v,\lambda}^{(k)}) \text{var}(W_{v,\lambda+M}^{(k)})}} \quad (20)$$

238 where  $K$  represents the time scale of the drought index. Assuming that the  
 239 cumulative rainfall  $Y$  and runoff  $X$  satisfy a normal distribution, after the standardization  
 240 process, the SPI value  $Z_{v,\lambda}^{(k)}$  corresponding to cumulative rainfall  $Y$  and SRI value  $W_{v,\lambda+M}$   
 241 corresponding to runoff  $X$  obey the standard normal distribution, namely:

$$242 \quad \text{var}(Z_{v,\lambda}^{(k)}) = \text{var}(W_{v,\lambda+M}^{(k)}) = 1 \quad (21)$$

243  $\text{cov}[Z_{v,\lambda}^{(k)}, W_{v,\lambda+M}^{(k)}]$  represents the covariance between the current SPI and the Sri  
 244 value with a forecast period of  $M$  months. The calculation is as follows:

$$245 \quad \text{cov}[Z_{v,\lambda}^{(k)}, W_{v,\lambda+M}^{(k)}] = \frac{1}{\sqrt{\sum_{i=0}^{k-1} \sigma_{\lambda+M-i}^2 \sum_{j=0}^{k-1} \sigma_{\lambda-j}^2}} \cdot \sum_{i=0}^{k-1} \sum_{j=0}^{k-1} \text{cov}[X_{v,\lambda+M-j}, Y_{v,\lambda-i}] \quad (22)$$

### 246 3.5 Conditional distribution model involving the $HI$ as an exogenous variable

247 According to the above conditional probability model, when considering the  $HI$  as  
 248 an exogenous variable, the model (Model 3) can be extended as follows:

$$249 \quad P\left[W_{v,\lambda+M} \in C_M \mid Z_{v,\lambda} = z_0, H_{v,\lambda} = h_0\right] = \int_{C_{Mi}}^{C_{Ms}} \frac{1}{\sqrt{2\pi}\sigma_z} e^{-\frac{1}{2}\left(\frac{x-\mu_z}{\sigma_z}\right)^2} dx \quad (23)$$

$$250 \quad \mu_z = E\left[W_{v,\lambda+M} \mid Z_{v,\lambda}, H_{v,\lambda}\right] = \Sigma'_{12} (\Sigma'_{22})^{-1} \begin{bmatrix} z_0 \\ h_0 \end{bmatrix} \quad (24)$$

---


$$251 \quad \sigma_z^2 = \text{var} \left[ W_{v,\lambda+M} \mid Z_{v,\lambda}, H_{v,\lambda} \right] = 1 - \Sigma'_{12} (\Sigma'_{22})^{-1} \Sigma'_{21} \quad (25)$$

252 where:

$$253 \quad \Sigma'_{12} = \left[ \text{cov}(W_{v,\lambda+M}, Z_{v,\lambda}) \quad \text{cov}(W_{v,\lambda+M}, H_{v,\lambda}) \right] \quad (26)$$

$$254 \quad \Sigma'_{22} = \begin{bmatrix} 1 & \text{cov}(Z_{v,\lambda}, H_{v,\lambda}) \\ \text{cov}(H_{v,\lambda}, Z_{v,\lambda}) & 1 \end{bmatrix} \quad (27)$$

$$255 \quad \Sigma'_{21} = (\Sigma'_{12})^T \quad (28)$$

### 256 3.6 Scoring mechanism

257 A scoring mechanism was applied to evaluate the performance of the drought  
 258 forecasting models. In this method, the monthly drought transition probability is  
 259 summed to evaluate the model (Chen et al., 2013), where  $p_{s,t}$  characterizes the  
 260 transition probability in month  $t$  of year  $s$ , and  $n$  is the length of the validation period.

$$261 \quad \text{Score} = \frac{1}{12n} \sum_{t=1}^{12} \sum_{s=1}^n p_{s,t} \quad (29)$$

## 262 4 Results and discussion

### 263 4.1 Nonstationarity analysis

264 In this paper, the area average monthly rainfall data of the Luanhe River basin  
 265 from 1961 to 2010 were obtained by spatial interpolation. The runoff data came from  
 266 the inflow runoff series of the Panjiakou Reservoir. Given the significance level  $\alpha = 0.05$ ,  
 267 the nonstationarity test results are shown in Figure 2.

268 Figure 2 (a) shows that the years of possible runoff change were 1979, 1996, 1997,  
 269 1998, and 1999. The P values in 1979 and 1998 were infinitely close to 1, which were  
 270 considered to be extremely significant runoff change points. Among all the possible  
 271 points satisfying  $t > t_\alpha$ , there were two maximum points (Figure 2 (b)), namely, 1979  
 272 and 1998, which were considered to be possible runoff change points. The final change  
 273 point needs to be judged based on the actual situation of the watershed.

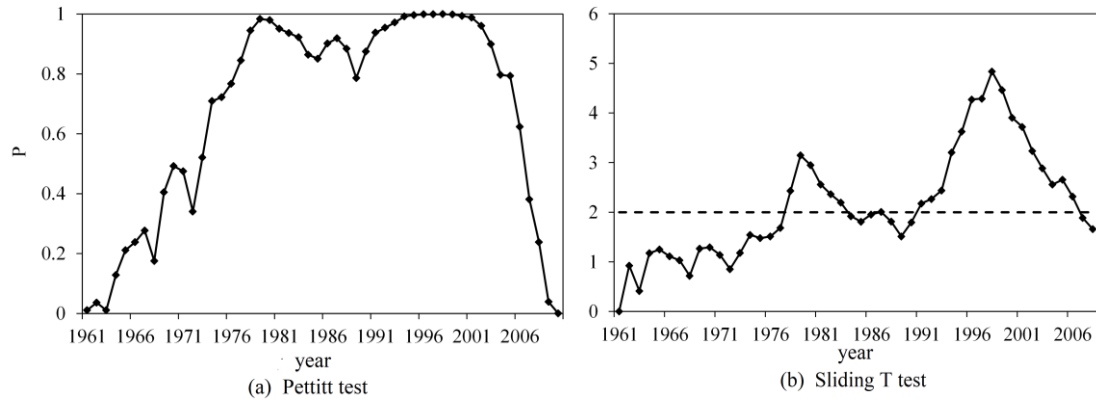


Figure 2 The change points of the runoff series

The results of the Spearman correlation test (Table 2) indicate that the runoff series showed an upwards trend before 1979, but the trend was not significant. However, there was a significant downwards trend in the series after 1979. In general, the runoff series showed a significant downwards trend.

Table 2 Spearman correlation test results of runoff series trend

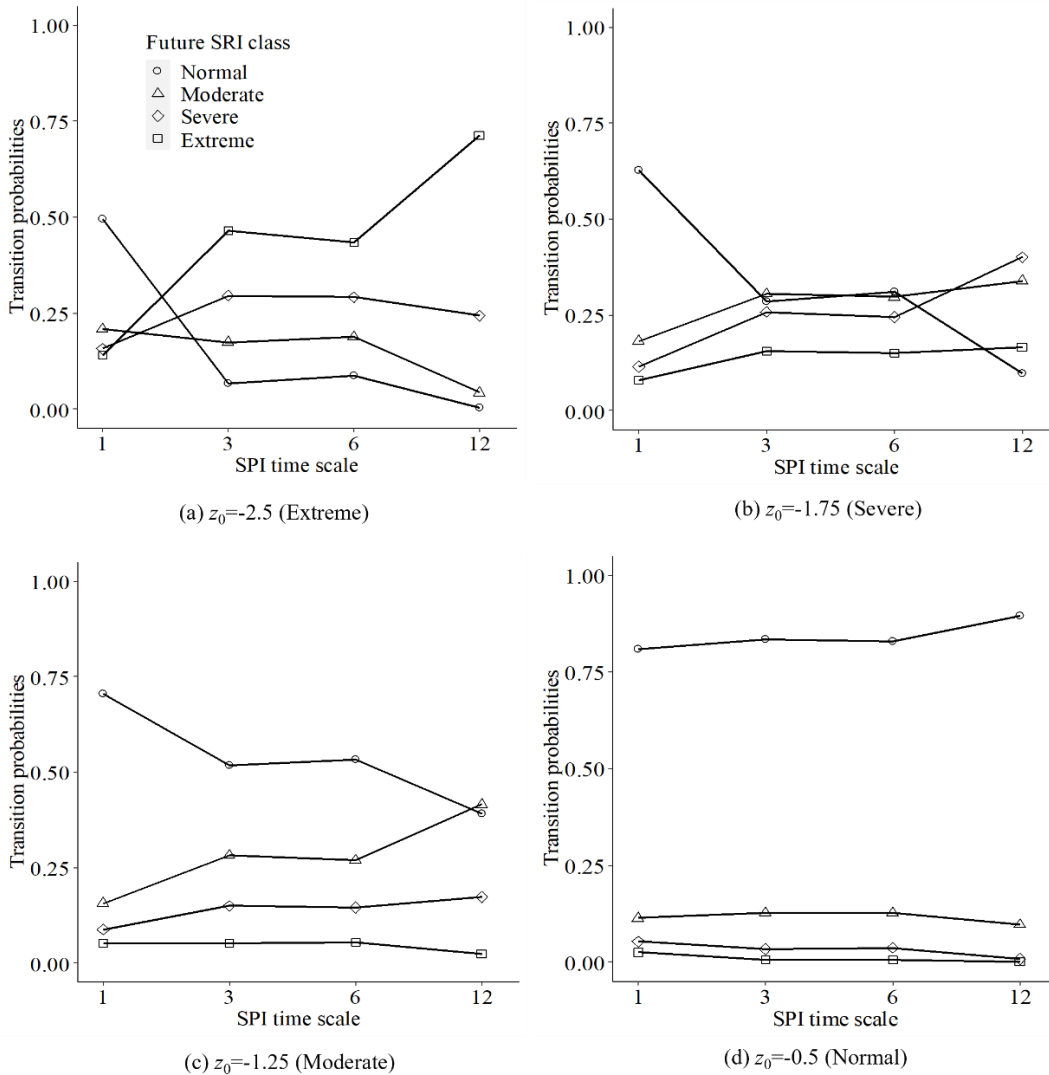
Runoff series	statistic $t$	Critical value $t_{\alpha}$
The whole series	-3.471	$\pm 2.009$
Series before 1979	0.691	$\pm 2.009$
Series after 1979	-2.292	$\pm 2.009$

In addition, according to historical records, local human activities (such as land use change and reservoir construction) are regarded as the main factors influencing runoff (Yan et al., 2018; Chen et al., 2021). Synthesizing the above analysis, 1979 was determined as the change point for the runoff sequence in the basin, and this conclusion was consistent with Li et al. (2015) and Wang et al. (2015).

#### 4.2 Transition probabilities from current SPI values to future SRI classes

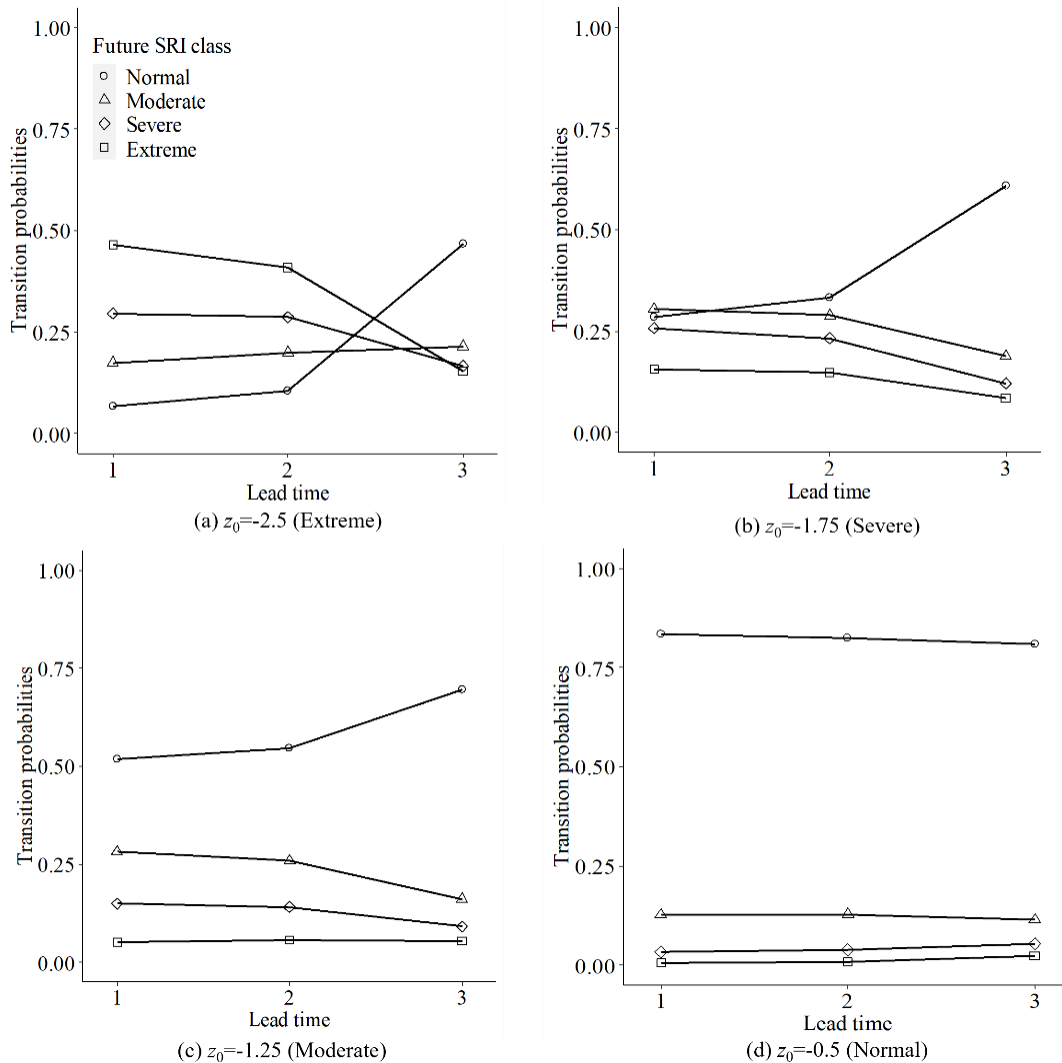
According to the normality test results of rainfall and runoff series, it was reasonable to apply the conditional distribution model. To analyse the influence of different time scales of the SPI on the transition probabilities, using the forecast period as one month and the SPI time scales at 1 month, 3 months, 6 months and 12 months as examples, the probabilities of converting SPI values to SRI classes were calculated (Figure 3).

294 As shown in Figure 3, when meteorological drought is categorized as extreme  
 295 drought, the probabilities of maintaining the SRI class in extreme drought increased  
 296 with the increasing SPI time scale. While the SPI had a short time scale, the response  
 297 of the future SRI class to rainfall was fast, so the hydrological drought was more likely  
 298 to tend to a normal status. This situation also occurred when the current meteorological  
 299 drought was in another status.



300  
 301 Figure 3 Influence of the SPI time scale on transition probabilities ( $z_0$  : initial value of SPI)  
 302 In addition, the transition probabilities of drought were distinct for different  
 303 forecast periods. As seen in Figure 4, when the forecast periods were short ( $M=1$  or  $2$ ),  
 304 the hydrological drought classes obtained from the transition of meteorological drought  
 305 tended to be the same as those of meteorological drought. With the extension of the

306 forecast period ( $M=2$  or  $3$ ), the hydrological drought classes obtained from the  
 307 transition tended to be lower than the meteorological drought or the normal status.



308  
 309 Figure 4 Influence of forecast period on transition probabilities ( $z_0$  : initial value of SPI)

### 310 4.3 Transition probabilities involving the *HI* as the covariate

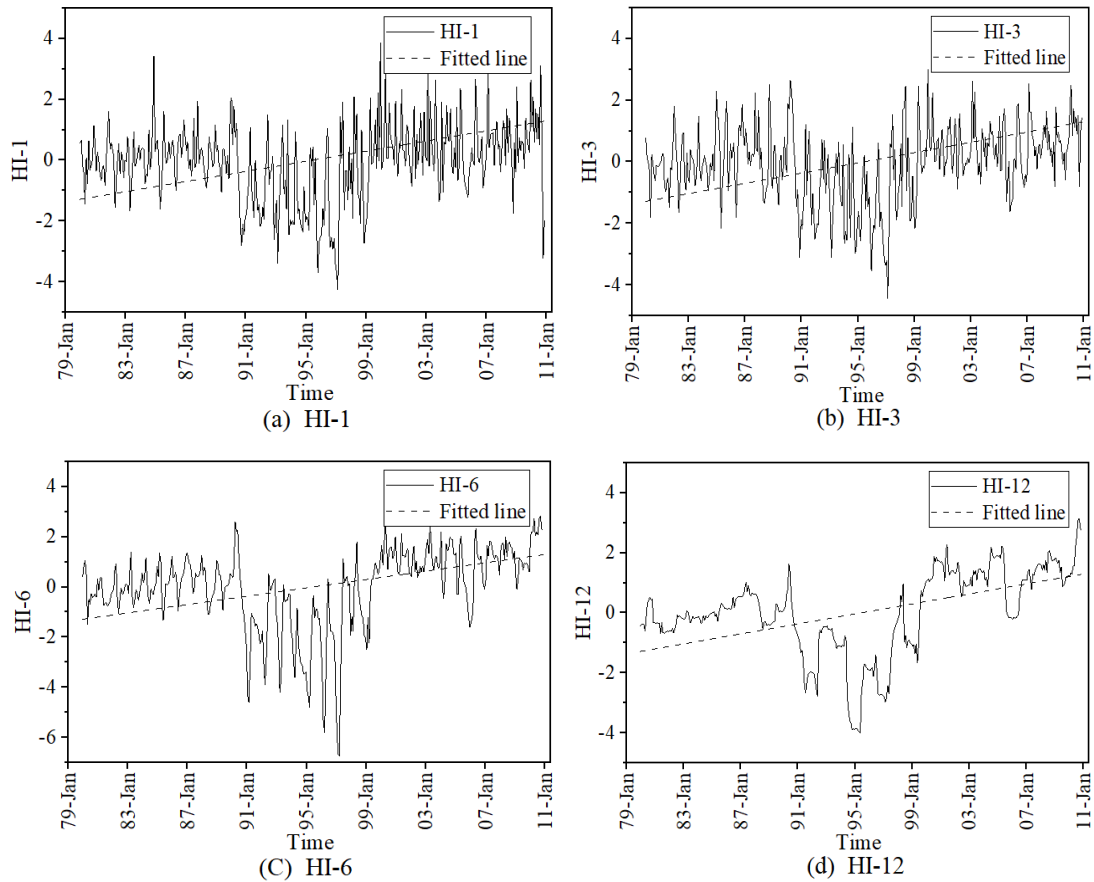
311 The effects of human activities are complex. To quantify the impact of human  
 312 activities, the change point was identified, and then it was believed that the difference  
 313 in the relationship between precipitation and runoff before and after the change point  
 314 was caused by human activities. Moreover, the *HI* is easy to calculate and can  
 315 approximately replace the influence of human activities. According to historical records,  
 316 local human activities (such as land use change and reservoir construction) were  
 317 regarded as the main factors influencing runoff (Yan et al., 2018; Chen et al., 2021).  
 318 According to the above nonstationarity test results, 1979 was the change point, and the

319 linear regression relationship of the cumulative rainfall and runoff series before and  
 320 after the change point was established. The calculation results are shown in Table 3:

321 Table 3 Linear regression relationship between cumulative precipitation ( $x / \text{mm}$ ) and cumulative  
 322 runoff ( $y / 10^6 \text{m}^3$ )

Period	Linear regression equation	Correlation coefficient
1961~1979	$x = 0.0276y + 2.7566$	0.99
1980~2010	$x = 0.0307y - 30.652$	0.98

323 The HI results for different time scales are shown in Figure 5.



324  
 325 Figure 5 Different average periods of the *HI* (*HI-1*: *HI* with a 1-month time scale; *HI-3*: *HI* with a  
 326 3-month time scale; *HI-6*: *HI* with a 6-month time scale; *HI-12*: *HI* with a 12-month time scale)

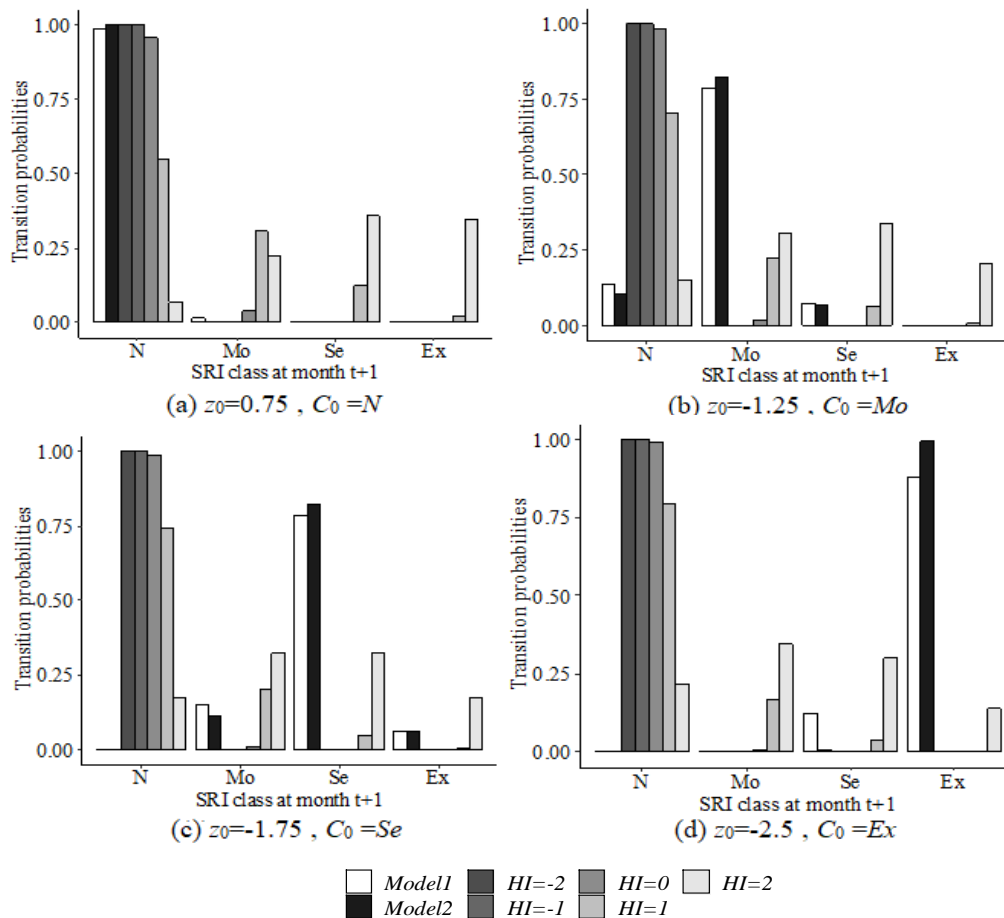
327 As shown in Figure 5, the *HI* at all monthly scales generally ranged upwards,  
 328 which means that human activities have intensified the occurrence of hydrological  
 329 drought. According to historical statistics, many water conservancy projects were built  
 330 in the basin from 1980 to 2000, and the construction and operation of large reservoirs  
 331 in the mid-1990s may be the main reason for the serious negative values of the *HI*.

332 The *HIs* of different monthly scales were standardized, taking the 12-month time  
 333 scale as an example, and the results were calculated as shown in Table 3.

334 Table 3 *HI*-12 monthly mean and standard deviation

	Jan	Feb	Mar	Apr	May	Jun	Jul	Aug	Sept	Oct	Nov	Dec
Mean	-0.04	-0.03	-0.03	-0.03	-0.03	0.00	0.06	0.06	0.10	0.10	0.09	0.06
Sd	1.36	1.37	1.38	1.41	1.41	1.51	1.40	1.40	1.45	1.44	1.44	1.43

335 Furthermore, the drought transition probabilities involving the *HI* can be  
 336 calculated from Eq. (23). Using the forecast period of one month from December and  
 337 the SPI time scale of 12 months as an example, the drought transition probabilities from  
 338 the current SPI values to the future SRI classes were calculated (Figure 6). To analyse  
 339 the effect of human activities on the drought transition probability more clearly, the  
 340 calculation results of the three models are compared here separately. The horizontal  
 341 coordinate indicates the drought classes corresponding to the SRI for the coming month,  
 342 and the vertical coordinate is the drought transition probability.



343

---

344 Figure 6 Drought transition probability under the influence of human activities ( $C_0$  denotes the  
345 initial drought class of the SPI in the multivariate normal model;  $z_0$  represents the initial value of  
346 the SPI in the conditional distribution model; Model 1: The normal distribution model; Model 2:  
347 The conditional distribution model; Model 3: The conditional distribution model involving the  $HI$ )

348 In Figure 6 (a), when the initial  $z_0=0.75$  and  $C_0=N$ , the results shown in Model 1  
349 and Model 2 were similar, and the probabilities of the SPI values transitioning to the  
350 SRI classes in the future month in the normal class were close to 1. However, the results  
351 of Model 3 indicated that the probabilities of maintaining the SRI in the normal class  
352 in the future decreased as the  $HI$  increased. When  $HI=2$ , the future hydrological drought  
353 classes were more likely to transition to severe drought or extreme drought.

354 From the initial  $z_0=-1.25$  and  $C_0=Mo$  (Figure 6 (b)), the results of Model 3 showed  
355 that the transition probabilities of the SPI values to a normal SRI class in the coming  
356 month were higher when the  $HI$  was less than 1. As the  $HI$  increased, the transition  
357 probabilities of the SPI values to a moderate drought or even a more severe drought in  
358 the future increased. In addition, the probabilities of maintaining moderate drought  
359 were the highest when human activities were not considered, and Model 2 showed a  
360 higher probability than Model 1.

361 While the initial meteorological drought class was severe drought (Figure 6 (c)),  
362 the probabilities of the future SRI drought class being in the normal class became larger  
363 as the  $HI$  decreased. When the effect of human activities was not considered, the  
364 probability that the current SPI value transitioned to the SRI class under severe drought  
365 in the future month was the highest, and the probability of being in the normal class  
366 was the lowest. For Model 2, the probability of the SRI classes transitioning to severe  
367 drought was higher than the result of Model 1.

368 It was noteworthy that when the initial  $z_0=-2.5$  and  $C_0=Es$  (Figure 6 (d)), the  
369 probabilities of transition of the SPI values to the future SRI classes at the normal class  
370 were close to 1 as  $HI<0$ . However, hydrological drought was more likely to be moderate  
371 drought or severe drought, as the  $HI$ s were greater than 0, and the transition  
372 probabilities exceeded 0.25. For Model 1 and Model 2, the probabilities of transition

---

373 of the current SPI values or classes to the future month SRI classes in extreme drought  
374 were both higher than 0.75, and Model 2 showed a higher probability than Model 1.

375 In general, for the evaluation of drought transition probabilities in the future month,  
376 hydrological drought classes tended to be the same as meteorological drought when  
377 human activities were not considered, and this situation was more significant in Model  
378 2 than in Model 1. The calculation results of the model involving the *HI* as an  
379 exogenous variable were significantly different from those of the models that did not  
380 consider human activities. The calculation results of Model 1 and Model 2 showed that  
381 the future hydrological drought classes were more likely to be the same as the  
382 meteorological drought classes in the current period, and they were more significant in  
383 Model 2. In addition, it was obvious that the drought transition probabilities of Model  
384 3 were significantly different from those of Model 1 and Model 2. Taking Figure 6 (b)  
385 as an example, when  $z_0 = -1.25$  and  $C_0 = Mo$ , the result of Model 1 showed that the  
386 probability of the SPI values transitioning to the SRI classes in the future month in the  
387 normal class was close to 0.15, the result of Model 2 was close to 0, and the result of  
388 Model 3 ( $HI=0$ ) was close to 0.95. The results of Model 3 ( $HI=0$ ) indicated that  
389 hydrological drought was likely to remain at the normal class in the future month.  
390 Moreover, the value of the *HI* had a great impact on the results of Model 3; for example,  
391 when  $HI = -2$  or  $-1$ , the probabilities of the SPI values transitioning to the SRI classes  
392 in the future month in the normal class were both close to 1, but the probability was  
393 close to 0.65 and 0.17 when  $HI = 1$  and  $2$ , respectively. The results further indicated that  
394 meteorological drought tended to turn into more severe hydrological drought with  
395 increasing *HI* values.

#### 396 4.4 Model evaluation and analysis

397 To quantitatively evaluate the prediction accuracy of Model 1, Model 2 and Model  
398 3, the study period was divided into a correction period (1961-2003) and a verification  
399 period (2004-2010), and then the drought transition probability from the SPI value or  
400 class to the SRI class in the future M-month was calculated. The calculation results are  
401 shown in Table 4.

402 With the same time scale of the SPI, the model scores of Model 1 and Model 2  
 403 decreased as the forecast period  $M$  lengthened, while the model scores of Model 3 were  
 404 not significantly affected by the forecast period  $M$ . Model 1 had the highest rating of  
 405 0.36 at an SPI of a 1-month time scale and a forecast period of one month; Model 2  
 406 reached the highest model rating of 0.74 at a 12-month time scale and a forecast period  
 407 of one month; and Model 3 performed well at an SPI of 1-month time scale and a 12-  
 408 month time scale. Overall, Model 3 had the highest rating, and Model 1 had the lowest  
 409 rating for the same SPI time scale and the same forecast period, which also indicated  
 410 that the forecast accuracy of the conditional distribution model considering the  $HI$  was  
 411 higher for short-term forecasts with a forecast period of 3 months or less, and including  
 412 the  $HI$  could further improve the forecast accuracy of the model.

413 Table 4 Model evaluation (Model 1: Multivariate normal distribution model; Model 2:  
 414 Conditional distribution model; Model 3: Conditional distribution model with the  $HI$ )

Model type	Lead time $M$	SPI time scale			
		1	3	6	12
Model 1	1	0.36	0.36	0.28	0.22
	2	0.11	0.35	0.27	0.22
	3	0.02	0.34	0.26	0.22
Model 2	1	0.69	0.52	/	0.74
	2	0.69	0.47	/	0.67
	3	0.69	0.44	0.39	0.60
Model 3	1	0.72	0.64	0.59	0.71
	2	0.71	0.64	0.59	0.71
	3	0.72	0.64	0.60	0.71

## 415 5 Conclusions

416 Many studies have noted that human activities have a significant impact on  
 417 watershed runoff in the Luanhe River basin. In this paper, three probability models were  
 418 constructed to calculate the transition probabilities from the current SPI classes or  
 419 values to the future SRI classes; then, a scoring mechanism was applied to evaluate the  
 420 performance of the models.

---

421 The calculation results of Model 1 and Model 2 showed that the future  
422 hydrological drought classes were more likely to be the same as the meteorological  
423 drought classes in the current period, and they were more significant in Model 2. In  
424 addition, it was obvious that the drought transition probabilities of Model 3 were  
425 significantly different from those of Model 1 and Model 2. Under the condition of  
426 considering the *HI*, the results of the drought transition probability showed that when  
427  $HI < 0$ , the future hydrological drought classes tended to normal status, and this situation  
428 was more obvious with the decrease in the *HI values*, which indicates that human  
429 activities mitigate the degree of hydrological drought when  $HI < 0$ . However, when  $HI > 0$ ,  
430 the future hydrological drought classes generally transitioned to more severe drought  
431 with increasing *HI values*. Thus, it was indicated that human activities exacerbate the  
432 degree of hydrological drought as  $HI > 0$ .

433 Finally, a scoring mechanism was applied to the evaluation of the models, and the  
434 forecast results of the three models were evaluated. The results demonstrate that when  
435 the SPI time scale was the same, the scores of Model 1 and Model 2 decreased as the  
436 forecast period lengthened. In most cases, Model 2 performed better than Model 1, and  
437 the performance of Model 3 was the most stable of the three models and had the highest  
438 score. The conditional probability model considering the *HI* was more suitable for the  
439 Luanhe River basin, where human activities have a high influence.

440 Although this study has made some progress in the forecasting of hydrological  
441 drought in a changing environment, only the *HI* was considered as the exogenous  
442 variable in this paper, and human activities were generalized. In future studies, the *HI*  
443 can be analysed specifically, for example, the impact of land use and socioeconomics,  
444 on drought prediction can be specifically analysed. In addition, climate factors can be  
445 further considered in future research.

446 **Ethical Approval:** This work meets the ethical and moral requirements.

447 **Consent to Participate:** M L., MF Z., RX C., YD S., and XY D. all agreed to  
448 participate in the research for the article.

449 **Consent to Publish:** M L., MF Z., RX C., YD S., and XY D. all agreed to publish this

---

450 article.

451 **Author Contributions:**

452 M L (First Author and Corresponding Author): Conceptualization, Methodology,  
453 Software, Investigation, Formal Analysis, Writing-Original Draft;

454 MF Z: Data Curation, Writing-Original Draft;

455 RX C: Visualization, Investigation;

456 YD S: Resources, Supervision;

457 XY D: Visualization, Writing-Review & Editing.

458 **Competing interest:** M L., MF Z., RX C., YD S., and XY D. all declare that there are  
459 no conflicts of interest.

460 **Data availability statement:** We are grateful to the Hydrology and Water Resource  
461 Survey Bureau of Hebei Province for providing runoff data. The data and materials of  
462 the research are available.

463

464 **References**

465 Abbasi, A., Khalili K., Behmanesh, J., and Shirzad, A.: Estimation of ARIMA model parameters  
466 for drought prediction using the genetic algorithm, *Arabian Journal of Geosciences.*, 14(10),  
467 841-841, <https://doi.org/10.1007/s12517-021-07140-0>, 2021.

468 Aghelpour, P., and Varshavian, Vahid.: Forecasting Different Types of Droughts Simultaneously  
469 Using Multivariate Standardized Precipitation Index (MSPI), MLP Neural Network, and  
470 Imperialistic Competitive Algorithm (ICA), *COMPLEXITY.*, 2021,  
471 <https://doi.org/10.1155/2021/6610228>, 2021.

472 Ahnadi, M.: Climatic drought forecasting using artificial neural network in Hamedan region,  
473 *New York Science Journal.*, 4(8),15-19, <https://doi.org/10.7537/marsnys040811.03>, 2011.

474 Alquraish, M. A., Abuhasel, K. S., and Alqahtani, A. K.: SPI-Based Hybrid Hidden Markov–  
475 GA, ARIMA–GA, and ARIMA–GA–ANN Models for Meteorological Drought Forecasting,  
476 *Sustainability.*, 13(22), 12576-12576, <https://doi.org/10.3390/su132212576>, 2021.

477 Behzad, A., and Hamid, M.: Revisiting hydrological drought propagation and recovery

---

478 considering water quantity and quality, *Hydrological Processes.*, 33(10), 1492-1505,  
479 <https://doi.org/10.1002/hyp.13417>, 2019.

480 Bishara, A. J., and Hittner, J. B.: Testing the significance of a correlation with nonnormal data:  
481 comparison of Pearson, Spearman, transformation, and resampling approaches, *Psychological*  
482 *methods.*, 17(3), 399-417, <https://doi.org/10.1037/a0028087>, 2012.

483 Bonaccorso, B., Cancelliere, A., and Rossi G.: Probabilistic forecasting of drought class transit  
484 ions in Sicily (Italy) using Standardized Precipitation Index and North Atlantic Oscillation Ind  
485 ex, *Journal of Hydrology.*, 526, 136-150, <https://doi.org/10.1016/j.jhydrol.2015.01.070>, 2015.

486 Carmelo, C., and Jürgen, V. V.: Non-stationarity in MODIS fAPAR time-series and its impact  
487 on operational drought detection, *International Journal of Remote Sensing.*, 40(4), 1428-1444,  
488 <https://doi.org/10.1080/01431161.2018.1524603>, 2018.

489 Chang, G. B., Zhang, S. B., and Liu, Z. P.: Understanding the adjustment from an information t  
490 heoretic perspective, *Geomatics and Information Science of Wuhan University.*, 2022,1-17, <https://kns.cnki.net/kcms/detail/42.1676.TN.20211125.1422.006.html>, 2022. (in Chinese)

491 Charles, O.: On Rigorous Drought Assessment Using Daily Time Scale: Non-Stationary  
492 Frequency Analyses, Revisited Concepts, and a New Method to Yield Non-Parametric Indices,  
493 *Hydrology.*, 4(4), 48-48, <https://doi.org/10.3390/hydrology4040048>, 2017.

494 Chen, J., Brissette, F. P., Chaumont, D., and Braun, M.: Performance and uncertainty evaluation  
495 of empirical downscaling methods in quantifying the climate change impacts on hydrology over  
496 two North American river basins, *Journal of Hydrology.*, 479, 200-214,  
497 <https://doi.org/10.1016/j.jhydrol.2012.11.062>, 2013.

498 Chen, X., Han, R. G., Feng, P., and Wang, Y. J.: Combined effects of predicted climate and land  
499 use changes on future hydrological droughts in the Luanhe River basin, China, *Natural Hazards.*,  
500 2021, 1-33, <https://doi.org/10.1007/s11069-021-04992-3>, 2021.

501 Ding, Y. B., Xu, J. T., Wang X. W., Cai, H.J., Zhou Z.Q., Sun Y.N., and Shi H.Y.: Propagation  
502 of meteorological to hydrological drought for different climate regions in China, *Journal of En*  
503 *vironmental Management.*, 283, 111980-111980, [80Get rights and content](https://doi.org/10.1016/j.jenvman.2021.1119), 2021.

504  
505  
506 Dixit, S., and Jayakumar, K. V.: A Non-stationary and Probabilistic Approach for Drought  
507 Characterization Using Trivariate and Pairwise Copula Construction (PCC) Model, *Water*

---

508 Resources Management., 2022, 1-20, <https://doi.org/10.1007/s11269-022-03069-5>, 2022.

509 Fuentes, I., Padarian J., Vervoort, R. W.: Spatial and Temporal Global Patterns of Drought Pro  
510 pagation, *Frontiers in Environmental Science.*, 2022,788248-788248, [https://doi.org/10.3389/f](https://doi.org/10.3389/fenvs.2022.788248)  
511 [envs.2022.788248](https://doi.org/10.3389/fenvs.2022.788248), 2022.

512 Zhao, G., Gao, H. L., Kao, S. C., Nathalie V., Bibi S. N.: A modeling framework for evaluating  
513 the drought resilience of a surface water supply system under non-stationarity, *Journal of*  
514 *Hydrology.*, 563, 22-32, <https://doi.org/10.1016/j.jhydrol.2018.05.037>, 2018.

515 Gong, H. N., Xie, B. T., Wang J. R.: Long-term prediction of extreme response of deepwater  
516 floating platform based on environmental contour method, *The Ocean Engineering.*, 39(05), 28-  
517 38, <https://doi.org/10.16483/j.issn.1005-9865.2021.05.003>, 2021. (in Chinese)

518 Kolachian, R., and Saghafian B.: Hydrological drought class early warning using support vector  
519 machines and rough sets, *Environmental Earth Sciences.*, 80(11), 390-390,  
520 <https://doi.org/10.1007/s12665-021-09536-3>, 2021.

521 Koudahe, K., Koffi, D., Kayode, J. A., Awokola, S. O., Adebola, A. A.: Impact of Climate  
522 Variability on Crop Yields in Southern Togo, *Environment Pollution and Climate Change.*, 2(1):  
523 1-9, <https://doi.org/10.4172/2573-458X.1000148>, 2018.

524 Li, J. Z., Wang, Y. X., Li, S. F., and Hu, R.: A Nonstationary Standardized Precipitation Index  
525 incorporating climate indices as covariates, *Journal of Geophysical Research: Atmospheres.*,  
526 120(23), 082-095, <https://doi.org/10.1002/2015JD023920>, 2015.

527 Li, L. C., Yao, N., Li, Y., Liu D. L., Wang, B., and Ayantobo, O. O.: Future projections of  
528 extreme temperature events in different sub-regions of China, *Atmospheric Research.*, 217,  
529 150-164, <https://doi.org/10.1016/j.atmosres.2018.10.019>, 2018.

530 Li, X., Fang, G. H., Wen, X., Xu, M., and Zhang, Y.: Characteristics analysis of drought at  
531 multiple spatiotemporal scale and assessment of CMIP6 performance over the Huaihe River  
532 Basin, *Journal of Hydrology: Regional Studies.*, 41, 101-103,  
533 <https://doi.org/10.1016/j.ejrh.2022.101103>, 2022.

534 Li, X. X., Ma, X. X., Li, X. D., and Zhang, W. J.: Method Consideration of Variation Diagnosis  
535 and Design Value Calculation of Flood Sequence in Yiluo River Basin, China, *Water.*, 12(10),  
536 2722-2722, <https://doi.org/10.3390/w12102722>, 2020.

---

537 Majid, D., Bahram, S., and Mansoor, Z.: Probabilistic hydrological drought index forecasting  
538 based on meteorological drought index using Archimedean copulas, *Hydrology Research.*,  
539 50(5), 1230-1250, <https://doi.org/10.2166/nh.2019.051>, 2019.

540 Malede, D. A., Agumassie, T.A., Kosgei, J.R., Linh, N. T. T., and Andualem, T. G.: Analysis of  
541 rainfall and streamflow trend and variability over Birr River watershed, Abbay basin, Ethiopia  
542 *Environmental Challenges.*, 7, 100528-100528, <https://doi.org/10.1016/J.ENVC.2022.100528>,  
543 2022.

544 Ganeshchandra, M., Shivam, T., Sergey, K., and Rao S. G.: Probabilistic Assessment of Drought  
545 Characteristics Using Hidden Markov Model, *Journal of Hydrologic Engineering.*, 18(7), 834-  
546 845. [https://doi.org/10.1061/\(ASCE\)HE.1943-5584.0000699](https://doi.org/10.1061/(ASCE)HE.1943-5584.0000699), 2013.

547 Maryam, M., Farzad, E., Nima, J. V., and Alireza, A.: Drought forecasting by ANN, ANFIS,  
548 and SVM and comparison of the models, *Environmental Earth Sciences.*, 76(21), 729-729,  
549 <https://doi.org/10.1007/s12665-017-7064-0>, 2017.

550 Mckee, T. B., Doesken, N. J., Kleist, J.: The relationship of drought frequency and duration to  
551 time scale, in: *Proceedings of the Eighth Conference on Applied Climatology*. American  
552 Meteorological Society, pp. 179–184. 1993.

553 Mehdi R., Alfred S., and Jonathan P. C.: Drought Forecasting using Markov Chain Model and  
554 Artificial Neural Networks, *Water Resources Management.*, 2016, 30(7), 2245-2259,  
555 <https://doi.org/10.1007/s11269-016-1283-0>, 2016.

556 Melanie, O., Francisco, J. M., Jorge, G., Christopher, A. S., Facundo, R., and Nicolás, P.:  
557 Drought Propagation in Semi-Arid River Basins in Latin America: Lessons from Mexico to the  
558 Southern Cone, *Water.*, 10(11), 1564-1564. <https://doi.org/10.3390/w10111564>, 2018.

559 Miriam, F., Tobias, G., Livia, L., Dana, V., Zuzana, D., Marián, F., and Pavla, P.: Analysing 21st  
560 century meteorological and hydrological drought events in Slovakia, *Journal of Hydrology and*  
561 *Hydromechanics.*, 66(4), 393-403, <https://doi.org/10.2478/johh-2018-0026>, 2018.

562 Mohammad, M. M., Abdol, R. Z., and Mohammad, R. M.: Seasonal drought forecasting in arid  
563 regions, using different time series models and RDI index, *Journal of Water and Climate*  
564 *Change.*,11(3), 633-654, <https://doi.org/10.2166/wcc.2019.009>, 2020.

565 Muhammad, J., Sabab, A.S., Jiyoung, Y., and Tae-Woong, K.: Investigating the impacts of  
566 climate change and human activities on hydrological drought using non-stationary approaches,

---

567 Journal of Hydrology., 588, 125052-125052, <https://doi.org/10.1016/j.jhydrol.2020.125052>,  
568 2020.

569 Natsagdorj, E., Renchin, T., Maeyer, P. D., and Darkhijav, B.: Spatial Distribution of Soil  
570 Moisture in Mongolia Using SMAP and MODIS Satellite Data: A Time Series Model (2010–  
571 2025), Remote Sensing., 13(3), 347-347, <https://doi.org/10.3390/RS13030347>, 2021.

572 Ren, W., Wang, Y., Li, J., Feng, P., and Smith R. J.: Drought forecasting in Luanhe River basin  
573 involving climatic indices, Theoretical and Applied Climatology., 130(3-4), 1133-1148,  
574 <https://doi.org/10.1007/s00704-016-1952-1>, 2017.

575 Shraddhanand, S., and Andrew, W. W.: Use of a standardized runoff index for characterizing  
576 hydrologic drought, Geophysical Research Letters., 35(2), 2405-1-2405-7,  
577 <https://doi.org/10.1029/2007GL032487>, 2008.

578 Stojković, M., Plavšić, J., Prohaska, S., Pavlović, D, and Despotović, J.: A two-stage time series  
579 model for monthly hydrological projections under climate change in the Lim River basin  
580 (southeast Europe), Hydrological Sciences Journal., 65(3), 387-400,  
581 <https://doi.org/10.1080/02626667.2019.1699241>, 2020.

582 Vicente-Serrano, S., Beguería, S., and López-Moreno, J.: A Multiscalar Drought Index  
583 Sensitive to Global Warming: The Standardized Precipitation Evapotranspiration Index, Journal  
584 of Climate., 23(7), <https://doi.org/10.1175/2009JCLI2909.1>, 2010.

585 Wang, M., Jiang, S., Ren, L., Xu, C-Y., Menzel, L., Yuan, F., Xu, Q., Liu, Y., Yang, X.:  
586 Separating the effects of climate change and human activities on drought propagation via a  
587 natural and human-impacted catchment comparison method, Journal of Hydrology., 603(PA),  
588 126913-123613, <https://doi.org/10.1016/J.JHYDROL.2021.126913>, 2021.

589 Wang, Y., Duan, L., Liu, T., Li, J., and Feng, P.: A Non-stationary Standardized Streamflow  
590 Index for hydrological drought using climate and human-induced indices as covariates, Science  
591 of the Total Environment., 699(C), 134278-134278,  
592 <https://doi.org/10.1016/j.scitotenv.2019.134278>, 2020.

593 Wang, Y., Li, J., Feng, P., and Hu, R.: Analysis of drought characteristics over Luanhe River  
594 basin using the joint deficit index, Journal of Water and Climate Change., 7(2), 340-352,  
595 <https://doi.org/10.2166/wcc.2015.108>, 2016.

---

596 Wang, Y., Li, J., Feng, P., and Chen, F.: Effects of large-scale climate patterns and human  
597 activities on hydrological drought: a case study in the Luanhe River basin, China, *Natural*  
598 *Hazards*, 76(3), 1687-1710, <https://doi.org/10.1007/s11069-014-1564-y>, 2015.

599 Wang, Y., Zhang, T., Chen, X., Li, J., and Feng, Ping.: Spatial and temporal characteristics of  
600 droughts in Luanhe River basin, China, *Theoretical and Applied Climatology*, 131(3), 1369-  
601 1385, <https://doi.org/10.1007/s00704-017-2059-z>, 2018.

602 Wang, Y., Peng, T., Lin, Q., Singh, V., Dong, X., Chen, C., Liu, J., Chang, W., and Wang, G.:  
603 A New Non-stationary Hydrological Drought Index Encompassing Climate Indices and  
604 Modified Reservoir Index as Covariates, *Water Resources Management*, 36(7), 2433-2454,  
605 <https://doi.org/10.1007/S11269-022-03151-Y>, 2022.

606 Xu, Y., Zhang, X., Wang, Xiao., Hao, Z., Singh, V., and Hao, F.: Propagation from  
607 meteorological drought to hydrological drought under the impact of human activities: A case  
608 study in northern China, *Journal of Hydrology*, 579(C), 124147-124147,  
609 <https://doi.org/10.1016/j.jhydrol.2019.124147>, 2019.

610 Yan, X., Bao, Z., Zhang, J., Wang, G., He, R., and Liu, C.: Quantifying contributions of climate  
611 change and local human activities to runoff decline in the upper reaches of the Luanhe River  
612 basin, *Journal of Hydro-environment Research*, 28(C), 67-74,  
613 <https://doi.org/10.1016/j.jher.2018.11.002>, 2018.

614 Zhang, T., et al.: Drought class transition analysis through different models: a case study in  
615 North China, *Water Science & Technology: Water Supply*, 17(1), 138-150,  
616 <https://doi.org/10.2166/ws.2016.123>, 2017.